

Twin families of bisolitons in dispersion-managed systems

Ildar Gabitov, Robert Indik, Linn Mollenauer, Maxim Shkarayev, and Misha Stepanov

Department of Mathematics, The University of Arizona, 617 N. Santa Rita Avenue, Tucson, Arizona 85721, USA

Pavel M. Lushnikov

Department of Mathematics & Statistics, MSC03 2150, University of New Mexico, Albuquerque, New Mexico 87131-1141, USA

Received October 2, 2006; accepted November 7, 2006;
 posted November 12, 2006 (Doc. ID 75593); published February 15, 2007

We calculate bisoliton solutions by using a slowly varying stroboscopic equation. The system is characterized in terms of a single dimensionless parameter. We find two branches of solutions and describe the structure of the tails for the lower-branch solutions. © 2007 Optical Society of America
 OCIS codes: 060.2310, 190.4370, 060.2330, 060.5530, 190.4380.

Bisolitons in optical fiber lines with dispersion management were first discovered by using computer modeling¹ and later were discovered experimentally.² The former were in-phase and the latter were anti-phase bisolitons, which can be viewed as two-component soliton molecules. In numerical simulations, they are stable over long propagation distances and, if perturbed, oscillate about equilibrium. Following the experimental work we investigate the structure of antiphase bisolitons, assuming that fiber losses are completely compensated and propagation of pulses through optical fiber in a dispersion-managed system is governed by the nonlinear Schrödinger equation

$$iu_z + d(z)u_{tt} + \gamma|u|^2u = 0, \quad (1)$$

where $u = u(t, z)$ is the slowly varying envelope of the electromagnetic field inside the fiber. We consider a simple case of a piecewise constant dispersion function $d(z)$, where a fiber span of length $z_{\text{dm}}/2$ with normal dispersion alternates with equal-length spans of anomalous dispersion fiber. The function $d(z)$ can be represented as a sum of an oscillating part $\tilde{d}(z)$ and a residual dispersion d_0 such that $d(z) = d_0 + \tilde{d}(z)$. Here $\langle \tilde{d}(z) \rangle = 0$; $\tilde{d}(z) = d_1$ if $0 \leq z \leq z_{\text{dm}}/2$, and $\tilde{d}(z) = -d_1$ if $z_{\text{dm}}/2 \leq z \leq z_{\text{dm}}$. In this system, the characteristic length of the nonlinearity is $z_{\text{nl}} \sim 1/\gamma P$, where P is the peak power of the bisoliton, while the characteristic length of the residual dispersion is $z_{d_0} \sim \tau^2/d_0$, where τ is the pulse width. The spectrum \hat{u} of the solution to Eq. (1) can be represented as

$$\hat{u} = q(\omega, z) \exp\left(-i\omega^2 \int_{z_{\text{dm}}/4}^z \tilde{d}(z') dz'\right), \quad (2)$$

provided that $z_{\text{dm}} \ll z_{\text{nl}}, z_{d_0}$. The exponential term captures the fast (in z) phase, and $q(\omega, z)$ captures the slow amplitude dynamics of the spectral components. As has been shown,³ the evolution of the spectral components at leading order can be described by

$$iq_z(\omega) - d_0\omega^2q(\omega) + \gamma R(q(\omega), \omega) = 0,$$

where

$$R(q(\omega), \omega) = \frac{1}{(2\pi)^2} \int \frac{\sin(s\Delta/2)}{s\Delta/2} q(\omega_1)q(\omega_2)q^*(\omega_3) \\ \times \delta(\omega_1 + \omega_2 - \omega_3 - \omega) d\omega_1 d\omega_2 d\omega_3. \quad (3)$$

Here $s \equiv z_{\text{dm}}d_1/2$ is dispersion map strength and $\Delta \equiv \omega_1^2 + \omega_2^2 - \omega_3^2 - \omega^2$. Higher-order corrections to this equation were considered in Ref. 4 to take into account the effect of dispersion map geometry on in-phase bisolitons. We determine a shape of a bisoliton solution following earlier work by Lushnikov.⁵ If a solitary wave solution with phase period λ^{-1} has the form $q(\omega) = A(\omega)e^{i\lambda z}$, then amplitude $A(\omega)$ evolves according to the following integral equation:

$$-\lambda A - d_0\omega^2 A + \gamma R(A(\omega), \omega) = 0. \quad (4)$$

Rescaling variables $t = \tau_0\tau$, $\omega = \Omega/\tau_0$, and $A(\omega) = a\varphi(\Omega)$, where $\tau_0 = s^{1/2}$ and $a = 2\pi(s\lambda/\gamma)^{1/2}$, results in a dimensionless equation

$$-(1 + \bar{d}_0\Omega^2)\varphi(\Omega) + \bar{R}(\varphi(\Omega), \Omega) = 0,$$

where

$$\bar{R}(\varphi(\Omega), \Omega) = \int \frac{\sin(\bar{\Delta}/2)}{\bar{\Delta}/2} \varphi(\Omega_1)\varphi(\Omega_2)\varphi^*(\Omega_3) \\ \times \delta(\Omega_1 + \Omega_2 - \Omega_3 - \Omega) d\Omega_1 d\Omega_2 d\Omega_3, \quad (5)$$

which depends on a single parameter $\bar{d}_0 = d_0/(s\lambda)$. Here $\bar{\Delta} = \Omega_1^2 + \Omega_2^2 - \Omega_3^2 - \Omega^2$.

We study the structure of antiphase bisolitons as a function of \bar{d}_0 . To solve this integral equation we use the following iterative procedure:

$$\varphi_{n+1}(\Omega) = P_{\text{odd}} \left(Q_n^{3/2} \frac{\bar{R}(\varphi_n(\Omega), \Omega)}{1 + \bar{d}_0 \Omega^2} \right). \quad (6)$$

Here $P_{\text{odd}}(f(x)) = (f(x) - f(-x))/2$ is a projection operator onto the set of odd functions and \hat{F}^{-1} is an inverse Fourier transform. A modified Petviashvili stabilizing factor⁶ Q_n ,

$$Q_n \equiv \left[\hat{F}^{-1}[\varphi_n(\Omega)] / \hat{F}^{-1} \left[\frac{\bar{R}(\varphi_n(\Omega), \Omega)}{1 + \bar{d}_0 \Omega^2} \right] \right]_{\tau=0.5},$$

allows the scheme to avoid trivial solutions $\varphi=0$. The most costly part of this iterative procedure is evaluation of \bar{R} , which involves a triple integral. To expedite evaluation of these integrals we used the procedure described by Lushnikov.⁵ It should be noted that the bisoliton solution of Eq. (5) represents the unchirped pulse shape at the middle of each span with positive dispersion.

We begin by studying the solutions for the parameter $\bar{d}_0=0.067$ (a realistic value for communication systems⁷), choosing φ_0 as a sum of two shifted real-valued Gaussian functions with opposite signs. The iteration procedure converges to the fixed point as the Petviashvili factor Q_n approaches 1. The iteration is stopped when $|Q_n - 1| < 10^{-5}$. The value of \bar{d}_0 was then varied in small increments. We use the solution found for the nearby \bar{d}_0 as the initial “guess” for the next value of \bar{d}_0 . Figure 1 represents bisoliton energy as function of \bar{d}_0 . Remarkably, this is a multiple-valued function with two branches. Calculation of solutions on this second branch required solution of the Arnoldi–Lanczos approximation problem for the linearization of iteration operator. Its limit point is located in the vicinity of $\bar{d}_{\text{obf}} \approx 0.426$. With all other parameters fixed, smaller values of \bar{d}_0 correspond to smaller values of residual dispersion. Therefore the

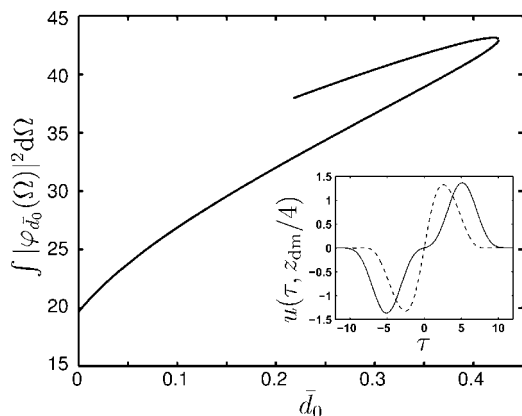


Fig. 1. Bisoliton energy as two valued functions of dimensionless residual dispersion \bar{d}_0 . Solid and dashed curves on inset correspond to the upper- and lower-branch bisolitons with $\bar{d}_0=0.256$. Horizontal and vertical axes on inset correspond to dimensionless time and amplitude.

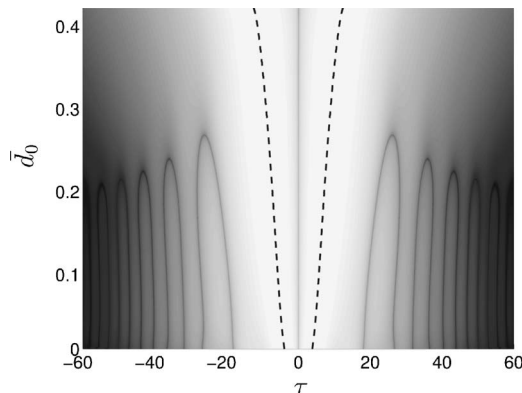


Fig. 2. The contour plot of $\log(|u|)$ as a function of time variable t and a parameter \bar{d}_0 . The dotted curves represent the peak amplitudes of solutions.

limit point corresponds to the largest value of d_0 for which bisolitons are supported. According to our calculations, for values of $\bar{d}_0 > \bar{d}_{\text{obf}}$ bisolitons will fail to exist, and we will observe only a pair of interacting dispersion-managed solitons that are not bound, not a bisoliton. The inset to the figure shows that the higher-energy bisoliton is wider, with greater separation and broader shape.

Direct numerical simulations demonstrate stability of both the lower and the upper-branch bisoliton solutions over realistic distances (1000 periods). For very long propagation distances, the upper branch showed signs of instability. Additionally, the pair of pulses composing the solution tends to stay bound whenever the pulses are pulled apart. The separation between the pulses spread apart in this manner oscillates about the separation for the bisoliton solution.

In the remainder of this Letter, we will discuss the structure of the lower-branch solutions. Details about the upper-branch solutions are the subject of ongoing work. The logarithmic density profile of lower-branch solutions’ amplitude for a range of values of \bar{d}_0 is shown in Fig. 2. There lighter shades of gray correspond to a higher value of the amplitude. The solid curves correspond to zero values. The dashed curves indicate where the solutions have their maxima. A horizontal slice of this plot gives an amplitude profile for a fixed value of \bar{d}_0 . For example, for a value of $\bar{d}_0=0.167$ the logarithm of amplitude is represented on Fig. 3. The dashed curve on the same graph represents the result of direct numerical simulations of Eq. (1) after 1000 dispersion map periods. A solution of Eq. (5) provided one boundary condition for this simulation (the launched pulse).

As we see in Fig. 2 bisoliton tails change sign for values of $\bar{d}_0 < \bar{d}_{\text{ocr}}$ ($\bar{d}_{\text{ocr}} \approx 0.269$). As the value of the dimensionless residual dispersion becomes greater than the critical value $\bar{d}_0 > \bar{d}_{\text{ocr}}$, the phase of the tails remains unchanged, and the amplitude approaches an exponentially decaying function. Our equation [Eq. (5)] reduces the many physical parameters from Eq. (1) to a single parameter. We have computed the bisolitons for a range of parameter values, and those

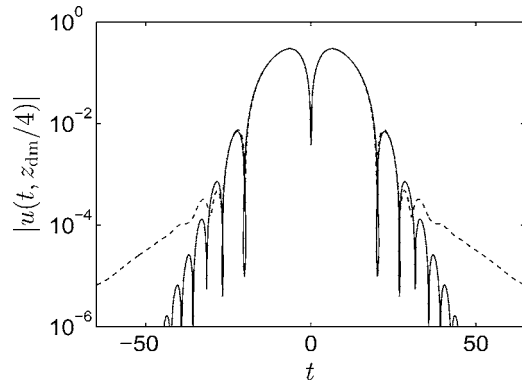


Fig. 3. Intensity profiles of a bisoliton with $\bar{d}_0=0.167$. Solution of Eq. (5) (solid curves) and a result of propagating this solution over 1000 periods through the line with $s=1.5$, $d_0=0.0125$, and $\lambda=0.05$ (dashed curves).

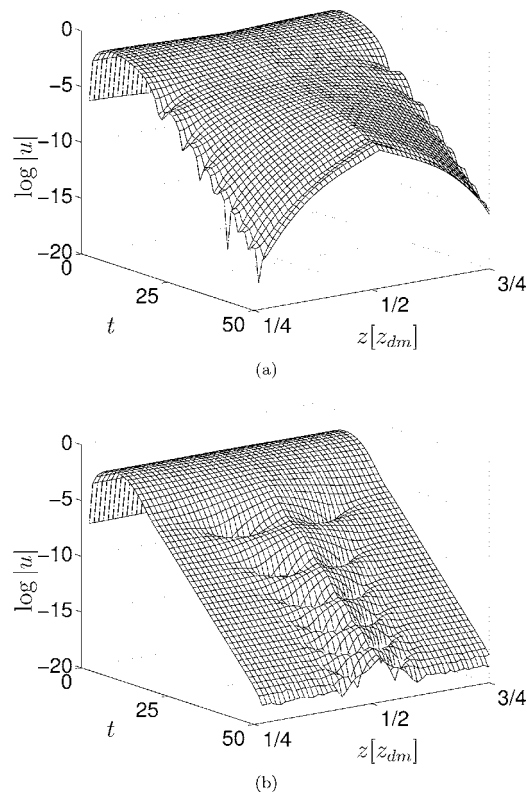


Fig. 4. Waveforms of a logarithm of the amplitude for bisoliton propagation through dispersion-managed system with $s=1.5$, $d_0=0.0125$, $\gamma=1$, (a) $\lambda=0.05$, and (b) $\lambda=0.02$. The soliton magnitude $|u|$ is symmetric. Bisolitons are propagated over half of the period, from $z_{dm}/4$ to $3z_{dm}/4$.

computed solutions can be used to write solutions of the original physical system

$$u(t, z_{dm}/4 + mz_{dm}) = \sqrt{\frac{\lambda}{\gamma}} \hat{F}^{-1} \left[\varphi_{\bar{d}_0 = \frac{d_0}{\lambda s}}(\Omega) \right] \Big|_{\tau=t/\sqrt{s}} \quad (7)$$

where it was convenient to specify the solution at $z_{dm}/4 + mz_{dm}$ because it is chirp free at this point.

We use $u(t, z_{dm}/4)$ of Eq. (7) as the initial condition in direct numerical simulation of Eq. (1) to study the dynamics of lower-branch bisoliton solutions for different values of \bar{d}_0 . In particular, we compare temporal-spatial behavior of solutions corresponding to values of $\bar{d}_{0cr} < \bar{d}_0 < \bar{d}_{0bf}$ and $0 < \bar{d}_0 < \bar{d}_{0cr}$ over a map period. We consider a system with $s=1.5$ and mean dispersion $d_0=0.0125$. Figures 4(a) and 4(b) represent propagation of the initial pulse with $\bar{d}_0=0.417$ and $\bar{d}_0=0.167$, respectively. For such choices of the system parameters, the values of phase periods λ must be 0.05 and 0.02.

The bisolitons for values of \bar{d}_0 above the critical value have no zeros other than at $\tau=0$ in their unchirped state, while if $\bar{d}_0 < \bar{d}_{0cr}$ the solution will have an increasing number of zeros with smaller \bar{d}_0 . The example in Fig. 4(b) shows that for larger values of \bar{d}_0 the local minima, which in Fig. 4(a) are at $z=z_{dm}/4$, split into pairs of minima, which are shifted toward $z_{dm}/2$. In fact, comparing the dynamics of $\bar{d}_0=0.417$ and $\bar{d}_0=0.167$ bisolitons indicates that the larger the value of \bar{d}_0 the more the minima will shift from the narrowest states (the valleys) of the pulse to its broadest state (the ridges).

In conclusion, we have used a slowly varying stroboscopic equation to calculate antiphase bisoliton solutions with well-resolved tails. This equation can be rescaled so that it has a single dimensionless parameter \bar{d}_0 . We have found a range of \bar{d}_0 such that there are two bisoliton solutions for each value of \bar{d}_0 . In addition, the structure of the tails for the lower-branch solutions was described in terms of the value of \bar{d}_0 .

This work was supported in part by Los Alamos National Laboratory under a LDRD grant, the National Nuclear Security Administration of the U.S. Department of Energy (DOE) under contract DE-AC52-06NA25396, the DOE Office of Science Advanced Scientific Computing Research Program in Applied Mathematics Research, and Proposition 301 funds from the State of Arizona. M. Shkarayev's e-mail address is maxim@email.arizona.edu.

References

1. A. Maruta, Y. Nonaka, and T. Inoue, *Electron. Lett.* **37**, 1357 (2001).
2. M. Stratmann, T. Pagel, and F. Mitschke, *Phys. Rev. Lett.* **95**, 143902 (2005).
3. I. Gabitov and S. K. Turitsyn, *Opt. Lett.* **21**, 327 (1996).
4. M. Ablowitz, T. Hirooka, and T. Inoue, *J. Opt. Soc. Am. B* **19**, 2876 (2002).
5. P. M. Lushnikov, *Opt. Lett.* **26**, 1535 (2001).
6. V. Petviashvili and O. Pokhotelov, *Solitary Waves in Plasmas and in the Atmosphere* (Gordon & Breach, 1992), p. 248.
7. L. F. Mollenauer and J. P. Gordon, *Solitons in Optical Fibers* (Academic, 2006).